

MET O 11 TECHNICAL NOTE NO 132

A test of the 10-level model initialisation scheme

by

R.W. Riddaway

Abstract

Experiments show that the initialised vertical velocity field is particularly poor in the vicinity of rain belts. Further investigations indicate that this is mainly caused by the neglect of the release of latent heat during the initialisation. Throughout a subsequent 12 hour forecast much of the detail lost during the initialisation is restored, but there remains some discrepancies in the rainfall rates and vertical velocities. It is estimated that the inadequacies of the initialisation scheme produce about a 10% error in the accumulated rainfall from the first 12 hours of the forecast.

Meteorological Office (Met O 11)
London Road,
Bracknell, Berkshire.
United Kingdom.
December 1979.

NB. This paper has not been published. Permission to quote from it must be obtained from the Assistant Director of the above Meteorological Branch.

FH2A

1. Introduction

Most initialisation schemes have two objectives

- (i) to derive a wind field (\underline{V} , w) from the geopotential field (ϕ)
- (ii) to produce a wind field which is essentially in balance with the mass field so as to minimise the excitement of gravity waves during the early part of a forecast.

We now consider the general procedure for deriving a wind field from ϕ so that these objectives are achieved. It is convenient to split \underline{V} into its rotational and divergent parts so that

$$\underline{V} = \underline{k} \times \nabla \psi + \nabla \chi$$

where ψ is the stream function and χ the velocity potential. If we incorporate this decomposition into the divergence equation (DE), ω -equation (WE), continuity equation (CE) and vorticity equation (VE) then these equations can be written schemmatically as follows

$$\nabla^2 \psi = F_1(\phi, \psi, \chi, \omega, \psi_e) \quad (\text{DE})$$

$$\nabla^2(\sigma\omega) + f^2 \frac{\partial^2 \omega}{\partial p^2} = F_2(\phi, \psi, \chi, \omega, \psi_e, \chi_e, \chi_{ee}) \quad (\text{WE})$$

$$\nabla^2 \chi = F_3(\omega) \quad (\text{CE})$$

$$\nabla^2 \psi_e = F_4(\psi, \chi, \omega) \quad (\text{VE})$$

Therefore there are four equations in the six unknowns $\psi, \chi, \omega, \psi_e, \chi_e$ and χ_{ee} , and so in order to solve this set of equations the number of unknowns must be reduced from six to four. This is achieved by neglecting the χ_e term in the divergence equation which then eliminates both χ_e and χ_{ee} from the set of equations; this set of elliptic equations can then be solved iteratively for

ψ, χ, ω and ψ_E once suitable boundary conditions have been imposed.

Hence for purely computational reasons the minimum approximation that must be made to the equations is to neglect the χ_E term in the divergence equation. Objective (1) can then be attained.

Now consider objective (ii). We know gravity wave activity is suppressed if we set $\frac{dD}{dt} = 0$ in the divergence equation. Doing this would then satisfy both the physical and computational constraints since making this assumption would also eliminate the χ_E term in the divergence equation. Therefore if we make the minimum approximations necessary to achieve objectives (i) and (ii) the following set of equations must be solved.

$$\nabla^2 \psi = F_1(\phi, \psi, \chi, \omega) \quad (DE)$$

$$\nabla^2(\sigma\omega) + f^2 \frac{\partial^2 \omega}{\partial p^2} = F_2(\phi, \psi, \chi, \omega, \psi_E) \quad (WE)$$

$$\nabla^2 \chi = F_3(\omega) \quad (CE)$$

$$\nabla^2 \psi_E = F_4(\psi, \chi, \omega) \quad (VE)$$

Pedersen (1969) solved this set of equations but he did not investigate the relative importance of all the terms that constitute the forcing functions (the F 's).

Krishnamurti (1968) carried out a similar analysis to Pedersen but used a simplified form of the divergence equation which is usually referred to as the non-linear balance equation (NLBE); this will be written as

$$\nabla^2 \psi = F_1(\phi, \psi) \quad (NLBE)$$

Once ψ has been computed the remaining three equations are solved iteratively for ω, χ and ψ_E . Krishnamurti analysed the relative importance of the terms which make up the forcing function F_2 of the ω -equation and found that the two most

important terms are the differential vorticity advection and the laplacian of the thermal advection. These findings are supported by a scale analysis of the ω -equation and are consistent with the form of the simple ω -equation that has been used in many investigations. Krishnamurti also included in the ω -equation those terms that are associated with surface friction and diabatic heating. He found that in some regions the heating due to the large scale release of latent heat could produce contributions to the vertical velocity that are comparable with those due to the two largest terms mentioned above. Hence neglecting the large scale heating could cause a serious underestimate of the vertical velocity. The only other forcing function that was ever large had its origins in the non-linear term of the balance equation.

The operational initialisation scheme used for the 10-level model uses the non-linear balance equation and an ω -equation whose forcing function consists of only the two major terms; the diabatic heating is not included. The forcing functions then only depend upon ϕ and ψ , and so it is not necessary to use the vorticity equation. Hence the equations used in the operational initialisation scheme may be written schemmatically as

$$\nabla^2 \psi = F_1(\phi, \psi) \quad (\text{NLBE})$$

$$\nabla^2(\sigma\omega) + f^2 \frac{\partial^2 \omega}{\partial p^2} = F_2(\phi, \psi) \quad (\text{WE})$$

$$\nabla^2 \chi = F_3(\omega) \quad (\text{CE})$$

The advantage of using these equations is that the forcing functions only depend upon ϕ , ψ and ω so that each equation only has to be solved once.

The purpose of this note is to investigate if the operational initialisation scheme has any serious deficiencies; particular attention will be paid to evaluating the importance of not including the effect of the large scale release of latent heat when computing ω and \underline{V}_x . Also we find that we can use the results from the experiments to estimate the error in the rainfall forecast due to the initialisation procedure

alone and this is then compared with the total rainfall error.

2. The basic approach

One way of investigating the effectiveness of the present scheme would be to use a more complicated initialisation scheme of the type described earlier and compare the two sets of results. However this would require a lot of extra programming and so an alternative approach is used.

The problem may be restated as follows - we want to know if the initialisation scheme is reasonably consistent with the full set of equations used in the forecast model. This can be tested by doing the following

- (i) perform a forecast from any given initial field - in our case a 12 hour forecast is used.
- (ii) use the forecast ϕ field as input to the initialisation scheme and compare the resulting wind field with that from the original forecast.

If we had a perfect initialisation procedure the original and initialised wind fields would be identical. Hence the magnitude of the differences between the wind fields are an indication of the effectiveness of the initialisation scheme. The advantage of this approach is that we have a "correct" wind field against which we can evaluate the initialised winds.

3. A preliminary study

Figure 1 shows the surface pressure field after a 12 hour forecast based on data from 00Z 5/1/78. The corresponding wind fields were decomposed into their non-divergent and irrotational parts (\underline{V}_ψ and \underline{V}_χ) by first deriving the streamfunction and velocity potential (ψ and χ) from the vorticity (ζ) and the divergence (D); the equations used are

$$\nabla^2 \psi = \zeta \qquad \nabla^2 \chi = D$$

$$\underline{V}_\psi = \underline{k} \times \nabla \psi \qquad \underline{V}_\chi = \nabla \chi$$

Examination of ψ and \underline{V}_ψ before and after initialisation shows only small differences. Therefore we can be confident that the operational initialisation scheme is capable of deriving the non-divergent component of wind reasonably well.

Figures 2a and 2b show an example of χ before and after initialisation. Comparison of these fields reveals that the initialisation scheme tends to reduce the magnitude of $\nabla\chi$ (indicated by the gradient of χ) and alter the position of the centres of convergence and divergence (indicated by where χ is a maximum or minimum); overall the initialised field is smoother than the original. This may represent a serious defect in the initialisation scheme because errors in the initial divergence fields will affect the development of surface features. Also, since the vertical velocity will be in error, there will be errors in the dynamic rainfall.

Now consider the vertical velocity field derived by integrating the continuity equation. Figures 3a and 3b show the 550 mb ω field before and after initialisation. Comparison of these again illustrates the inadequacies of the initialisation scheme. For example, note that in the initialized ω field there is

- (i) hardly any ascent associated with the cold front in the Central Atlantic.
- (ii) a marked underestimate of the vertical velocity in the vicinity of the warm front to the south of Iceland.
- (iii) a much reduced area of ascent associated with the rainbelt over Norway.
- (iv) an underestimate of the ascent in the low pressure area to the southwest of Greenland.

Overall the initialisation procedure tends to produce a reasonable distribution of ascent and descent, but the fields are very smooth; in particular in the vicinity of rainbelts the vertical motion is much less than it should be.

In order to understand why we have such poor initialized ω fields we must recall the work of Krishnamurti described earlier. He showed that the part of the vertical velocity arising from the large scale release of latent heat could be as large as those parts due to the differential vorticity advection and the laplacian of the thermal advection. Since the version of the ω -equation used in the operational scheme only includes these last two terms it appears likely that its poor performance could be due to the neglect of the large scale release of latent heat. The plausibility of this suggestion is enhanced by the fact that the most marked underestimate of the ascent

is in the vicinity of rain belts.

Before proceeding we should consider the effect of ignoring the only other term in the ω -equation identified by Krishnamurti as giving a sizeable contribution to the vertical velocity - this term may be written as

$$-2 \frac{\partial}{\partial t} \frac{\partial}{\partial p} J\left(\frac{\partial \psi}{\partial x}, \frac{\partial \psi}{\partial y}\right)$$

This is a rather difficult term to interpret but Krishnamurti argued that in the vicinity of intensifying frontal zones it should make a large contribution to the ascent. However it seems unlikely that the neglect of this term could be responsible for the consistent underestimate of the ascent near rain belts. Therefore we will concentrate upon the effects of neglecting the large scale release of heat when computing the vertical velocity.

4. A corroborating experiment

In the previous section it was suggested that the main reason for the poor quality of the vertical velocity fields resulting from the initialisation was due to the neglect of the release of latent heat. One way of confirming this is to run a dry 12 hour forecast and then use the forecast geopotential field as input to the initialisation scheme. If the initialised vertical velocity field is similar to the original field then this would support the idea that it is the release of latent heat which is causing the problems. This experiment was carried out.

Figure 4a shows the vertical velocity field of the 12 hours of a "dry" forecast and comparison of this with the corresponding "wet" forecast (Figure 3a) illustrates the importance of the release of latent heat. The vertical velocity field resulting from the initialisation of the "dry" forecast geopotential is given in figure 4b. Overall the vertical velocity fields shown in these figures are similar although once again there is a tendency for the initialisation to underestimate the magnitude of the ascent. However the differences between these fields are not nearly as marked as between the corresponding fields for the "wet" case - see figures 3a and 3b. Therefore this experiment suggests that the present operational initialisation scheme is capable of producing reasonable vertical velocity fields when there is no release of latent heat.

5. A further test

Normally when an initialisation is performed we have no knowledge of the release of latent heat, but in our experiment there is no such constraint since the latent heat release is computed during the dynamic rain calculations. However the forecast programs were such that the output from the "physics" routines was the combined change in temperature (ΔT) during a time step (Δt) due to large scale condensation, convection and surface exchanges. It would be difficult to separate these different effects but it is reasonable to assume that ΔT is dominated by the effects of large scale condensation; hence the heating due to the large scale release of latent heat (H) is given approximately by

$$H = C_p \frac{\Delta T}{\Delta t}$$

Once H is known we can calculate the contributions to the vertical velocity of this release of latent heat (ω_L) by solving

$$\nabla^2(\sigma\omega_L) + f^2 \frac{\partial^2 \omega_L}{\partial p^2} = -\frac{R}{pC_p} \nabla^2 H \quad \text{with } \omega_L = 0 \text{ on the boundary}$$

Figure 5a shows ω_L computed from the values of H derived from the last time step of the original 12 hour forecast. This is now compared with Figure 5b which shows the difference between the original (Figure 3a) and initialised (Figure 3b) fields. The similarity between figures 5a and 5b is another indication that it is the exclusion of the release of latent heat when computing the initial ω field that is responsible for a large part of the error shown in figure 5b. However there are still some errors that have not yet been explained; for example, even taking ω_L into account, ω is still underestimated in the four main areas of ascent and also in the subsidence area in the vicinity of Scotland.

6. The effect on the forecasts

We now consider the effect of the initialisation on the forecast. This is investigated by running a 12 hour forecast from both the original and initialised fields; these forecasts are shown in figures 6a and 6b. If the initialisation was

perfect the two forecasts would be identical. From the results we see that, although the fields are similar, there are some significant differences. For example, the forecast from the initialised field has deepened the lows near Iceland and Cape Farewell too much and has increased the intensity of the high near Newfoundland.

The rates of dynamic rain at the end of the forecast are shown in Figures 7a and 7b. The overall distribution of rain is similar although again there are differences in the detail. In particular the forecast from the initialised field underestimates the rainfall rate near Iceland by about 25% and produces an overestimate in the northern North Sea. Also the rainfall associated with the cold front in the Atlantic is underestimated. These differences are reflected in the 550 mb fields shown in figures 8a and 8b. Clearly the forecast itself has generated much of the detail lost in the initialisation, but even after 12 hours the vertical velocity fields have not entirely recovered.

Finally it is worth examining the overall effect of the initialisation on the rainfall. Figures 9a and 9b show the accumulated dynamic rain from the two forecasts. Again the general distributions are similar but the initialisation has caused a general reduction in the amount of dynamic rain. For example the rainfall maxima in the Davis Straite and the Central Atlantic have been reduced by about 25%; elsewhere the reduction tends to be less than this. These comments are also applicable when the total accumulated rainfalls (ie dynamic plus convective) are compared.

7. Discussion

In these experiments we have investigated the effectiveness of the operational initialisation scheme for deriving wind fields. In particular we have concentrated upon the vertical velocity fields and have shown that the initialisation produces smooth fields which are particularly poor near rain areas. Further experiments indicated that it was the neglect of the release of latent heat when calculating the ω fields that was responsible for this degradation. The effect of the initialisation on the subsequent 12 hour forecast was then examined. It was found that much of the detail lost during initialisation was regenerated during the forecast

We now consider what remedies might be used to improve the initialisation scheme - particularly with respect to the treatment of the large scale release of latent heat. Following Krishnamurti (1968) it could be assumed that, if the air is both saturated and ascending, the release of latent heat is given by

$$H = -L\omega \frac{\partial \Gamma_s}{\partial p} \quad \text{when } \Gamma = \Gamma_s \text{ and } \omega < 0$$

However we know that the analysed relative humidities seldom have areas of saturation because of a combination of the inability of the radio-sonde to record 100% relative humidities and the smoothing inherent in the analysis scheme. Therefore introducing the above formulation of it is unlikely to have any significant effect. One way of overcoming this problem is to follow Danard (1966) and introduce a factor which will allow latent heat release when the air is not completely saturated; we then have

$$H = -\alpha L\omega \frac{\partial \Gamma_s}{\partial p} \quad \text{when } \omega < 0$$

We can interpret α as simply being the fraction of a grid box that is saturated (ie the fractional cloud volume) or as an empirical factor which allows us to take into account the inadequacies of the analysed relative humidity field. Danard used the first interpretation and assumed α depended upon the characteristic dew point depression (ΔT_d) in a column of the atmosphere; he then used

$$\alpha = \begin{cases} 1 - \Delta T_d / 7.5 & \Delta T_d < 7.5^\circ\text{C} \\ 0 & \Delta T_d \geq 7.5^\circ\text{C} \end{cases}$$

Alternatively we could use one of the many other empirical expressions which attempt to relate the cloud cover to the relative humidity. If the second interpretation of α is used then we can choose α to produce the best possible results. For example we might assume that the real atmosphere is likely to be saturated if the analysed relative humidity is greater than some threshold χ_c so that

and that overall the final distribution of vertical velocity and rainfall was largely unaffected by the adverse effects of the initialisation. However the initialisation did cause underestimates of up to about 30% in the maxima of rainfall and ascent at the end of the forecast.

In these experiments we have only considered errors induced by the initialisation scheme. However in an operational forecasting system there will also be errors introduced by inadequacies in the analysis. In particular the analysed relative humidities tend to be rather smooth and seldom, if ever, reach 100% in cloudy areas. This will cause an underestimate of the ascent in the vicinity of fronts and depressions in the early part of the forecast because it will take some time for saturation to be reached and the subsequent enhancement of the vertical velocity due to the release of latent heat. Therefore the inadequacy of the humidity analysis will result in an underestimate of the rainfall during the first part of the forecast.

The above discussion indicates that both the analysis and initialisation schemes produce an underestimate of the rainfall at the start of the forecast. This is supported by results of Jonas (1976) and Riddaway (1978) when they investigated various condensation schemes. They examined the area average of the 6 hourly rainfall accumulations throughout a 36 hour forecast. It was found that it took about 12 hours for those average accumulations to become almost constant with time. If this constant value is taken as an indication of what the rainfall should be during the early part of the forecast then the deficit during the first 12 hours is about 20%. When the dynamic rain is considered separately the deficit is about 30%. For the one case considered in this present investigation the effect of the initialisation alone on the total and dynamic rainfall is to produce deficits of about 10% and 15% respectively. Therefore these results suggest that the analysis and initialisations procedures contribute almost equally to the deficit in rainfall during the early part of the forecast. However many more experiments would have to be carried out before we could be certain about this.

$$\alpha = \begin{cases} 1 & \chi > \chi_c \\ 0 & \chi \leq \chi_c \end{cases}$$

We then perform experiments to find the value of χ_c which produces the best results.

An alternative approach to this problem comes from the work of Riddaway (1978) who considered various subgridscale condensation schemes that were based on the idea that cloud could occupy just part of a grid box. This meant that it was possible for condensation, and the subsequent release of latent heat, to take place before a grid box was completely saturated. Hence latent heat was released earlier in the forecast than when the traditional condensation scheme is used. Therefore, although the use of this scheme does not improve the initialised fields, it does help compensate for the underestimated ω fields by feeding into the wind fields information about the release of latent heat earlier than is done at present.

So far we have only considered the release of latent heat. Although this is probably the most important of the neglected terms, and the easiest to include in the current operational scheme, it should be noted that either of the systems of equations used by Pedersen or Krishnamurti would give better balanced winds than we have at present. However it is unlikely that doing this will give any substantial benefits.

Undoubtedly the best way of reducing errors associated with initialisation is to remove the initialisation step entirely and use 4-dimensional data assimilation. However, until a scheme of this kind is available for the operational mode, either of the methods described above could be regarded as being a reasonable short term expedient.

- Darard, M.B. 1966 "A quasi-geostrophic numerical model incorporating effects of release of latent heat".
J. Appl. Met., 5, 85-93.
- Jonas, P.R. 1976 "A revised parameterisation of the condensation and precipitation processes for use in numerical forecasting models".
Met O 11 Tech Note No. 67.
- Krishnamarti, T.N. 1968 "A study of developing wave cyclone".
M.W.R., 99, 208-217.
- Pedersen, K and 1969 "A method of initialisation for dynamic weather
Gronskei, K. forecasting, and a balanced model".
Geofus. Publikasjoner, 27, No. 7.
- Riddaway, R.W. 1978 "An investigation of various subgrid scale condensation schemes.
Met O 11 Tech Note No 122.

FORECAST SURFACE PRESSURE AND PRECIPITATION

12 HOUR FORECAST, DATA TIME=0Z 5/1/78, VERIFICATION TIME=12Z 5/1/78

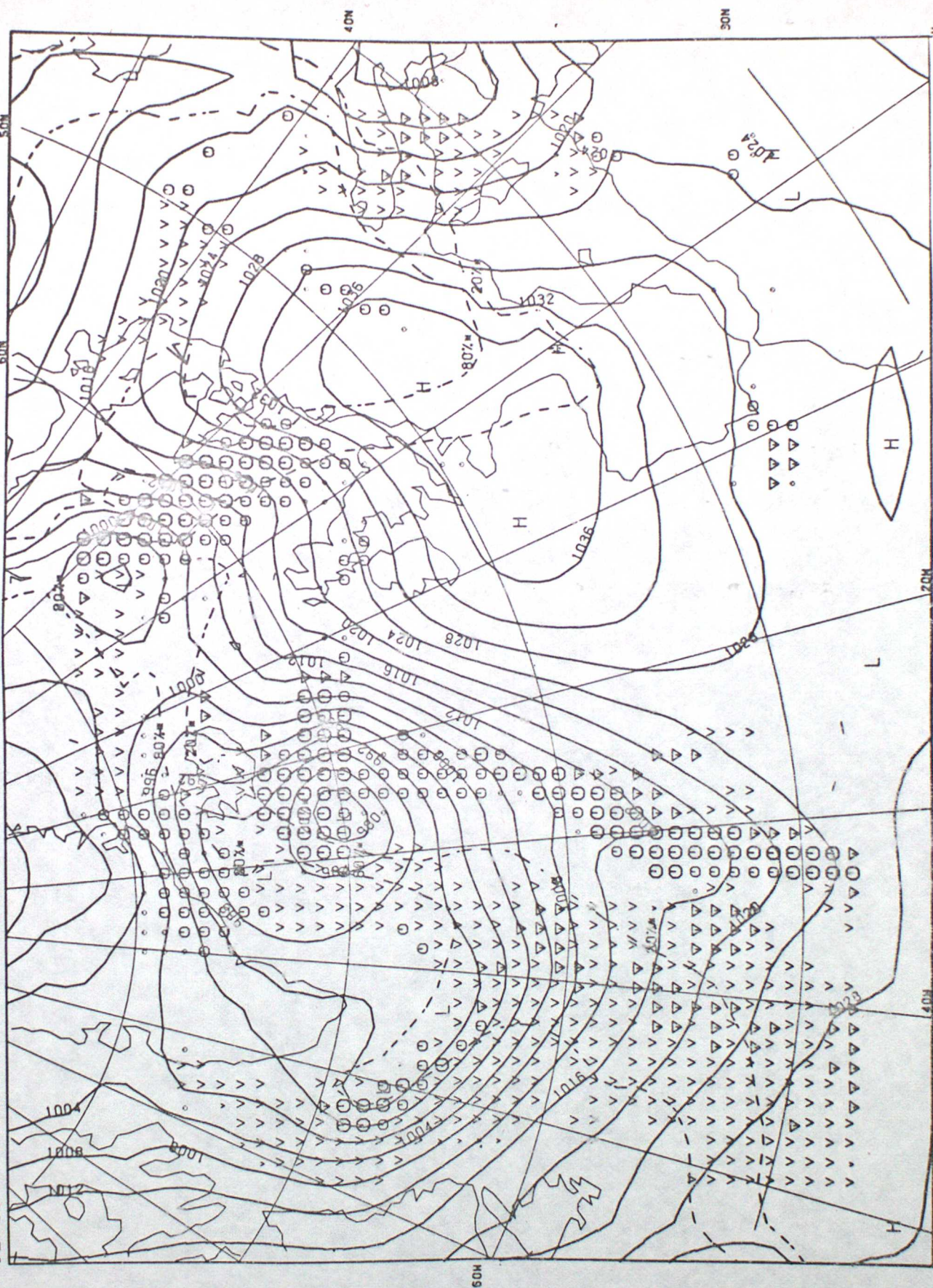


Figure 1 - a 12 hr forecast valid at 12Z 5/1/78

VELOCITY POTENTIAL
12HR FC PRE-INITIAL 300MB



Figure 2a- velocity potential (X) at 300 mb before initialisation

VELOCITY POTENTIAL
12HR FC POST-INITIAL 300MB

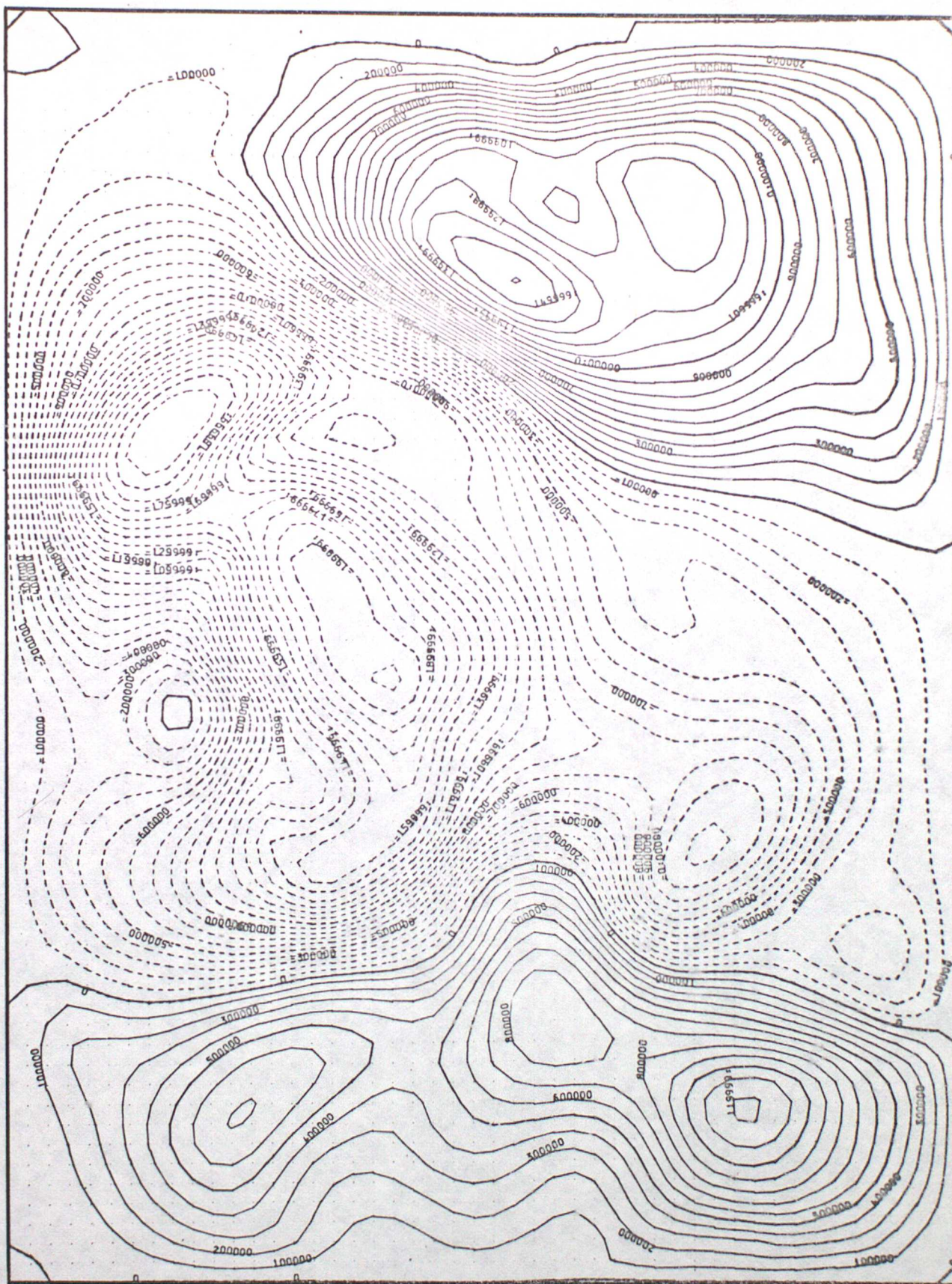


Figure 2b - velocity potential (X) at 300 mb after initialisation

500MB VERT VEL. ISOPLETH INTERVAL=10 MB/HR

12 HOUR FORECAST, DATA TIME=0Z 5/1/78, VERIFICATION TIME=12Z 5/1/78

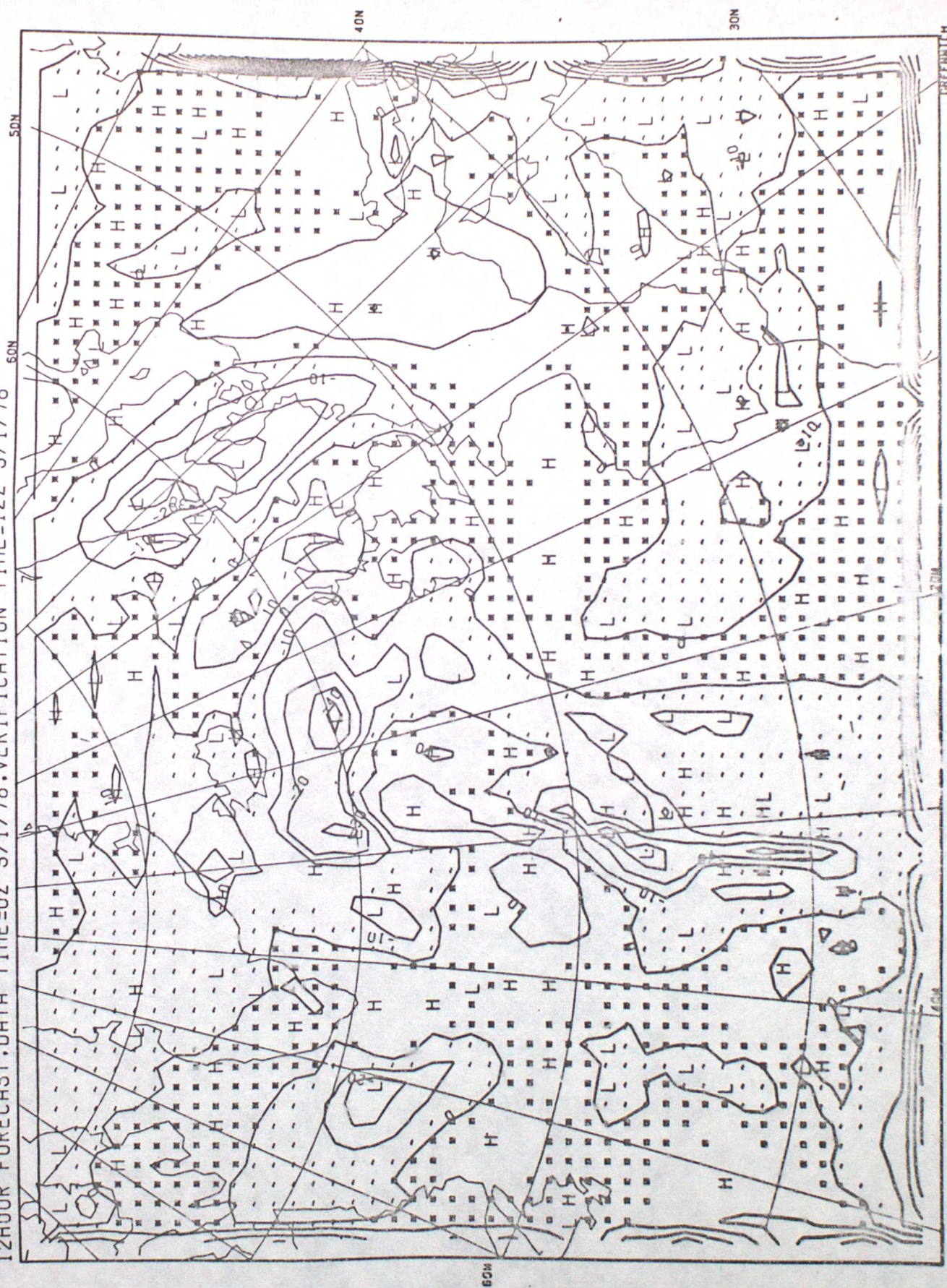


Figure 3a - the 550 mb w field before initialisation

500MB VERT VEL. ISOPLETH INTERVAL=10 MB/HR

0000R FORECAST DATA TIME=12Z 5/1/78. VERIFICATION TIME=12Z 5/1/78

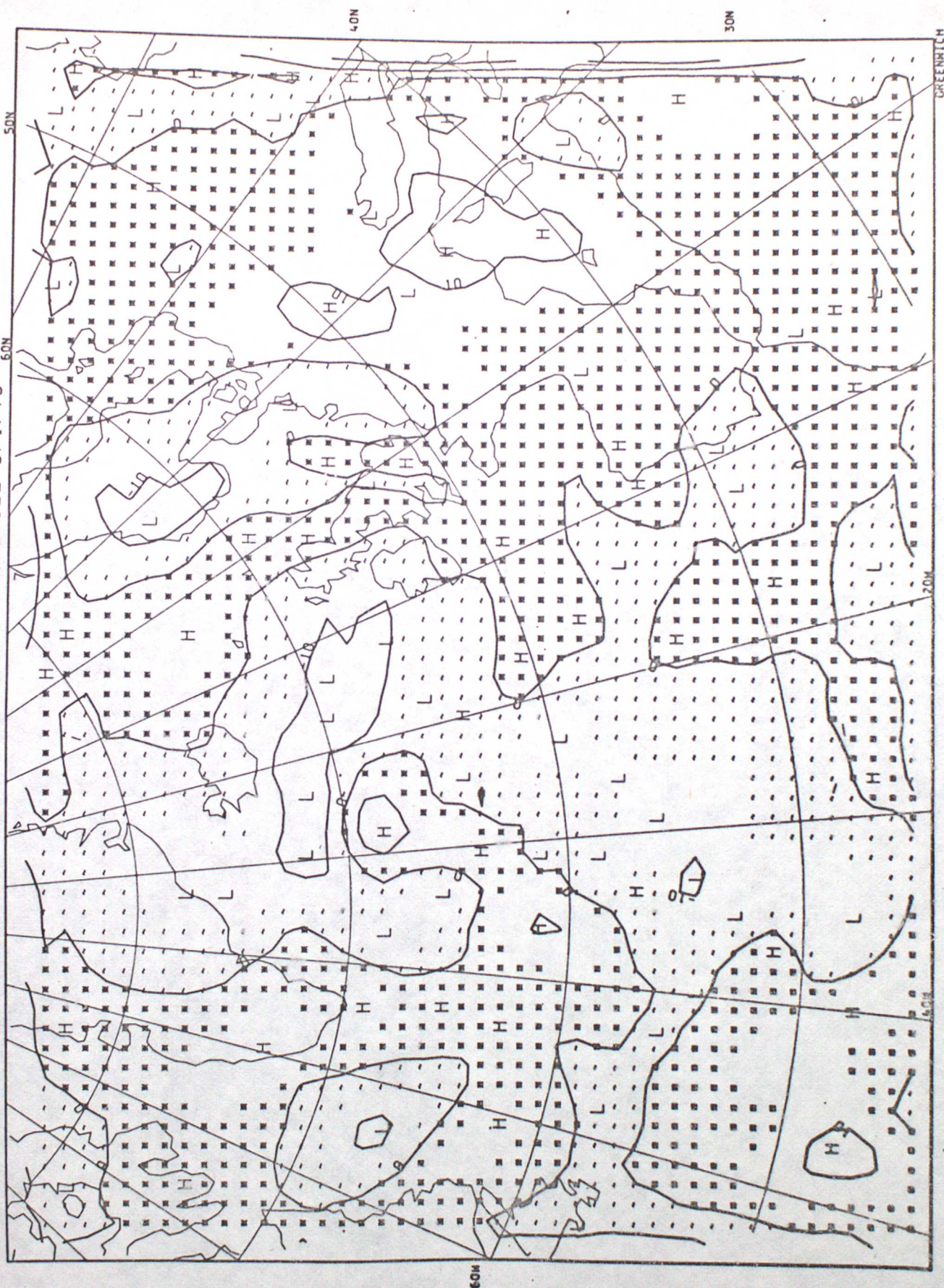


Figure 3b - The 550mb w field after initialisation

500MB VERT VEL. ISOPLETH INTERVAL=10 MB/HR

12HOUR FORECAST, DATA TIME=0Z 5/1/78, VERIFICATION, TIME=12Z 5/1/78

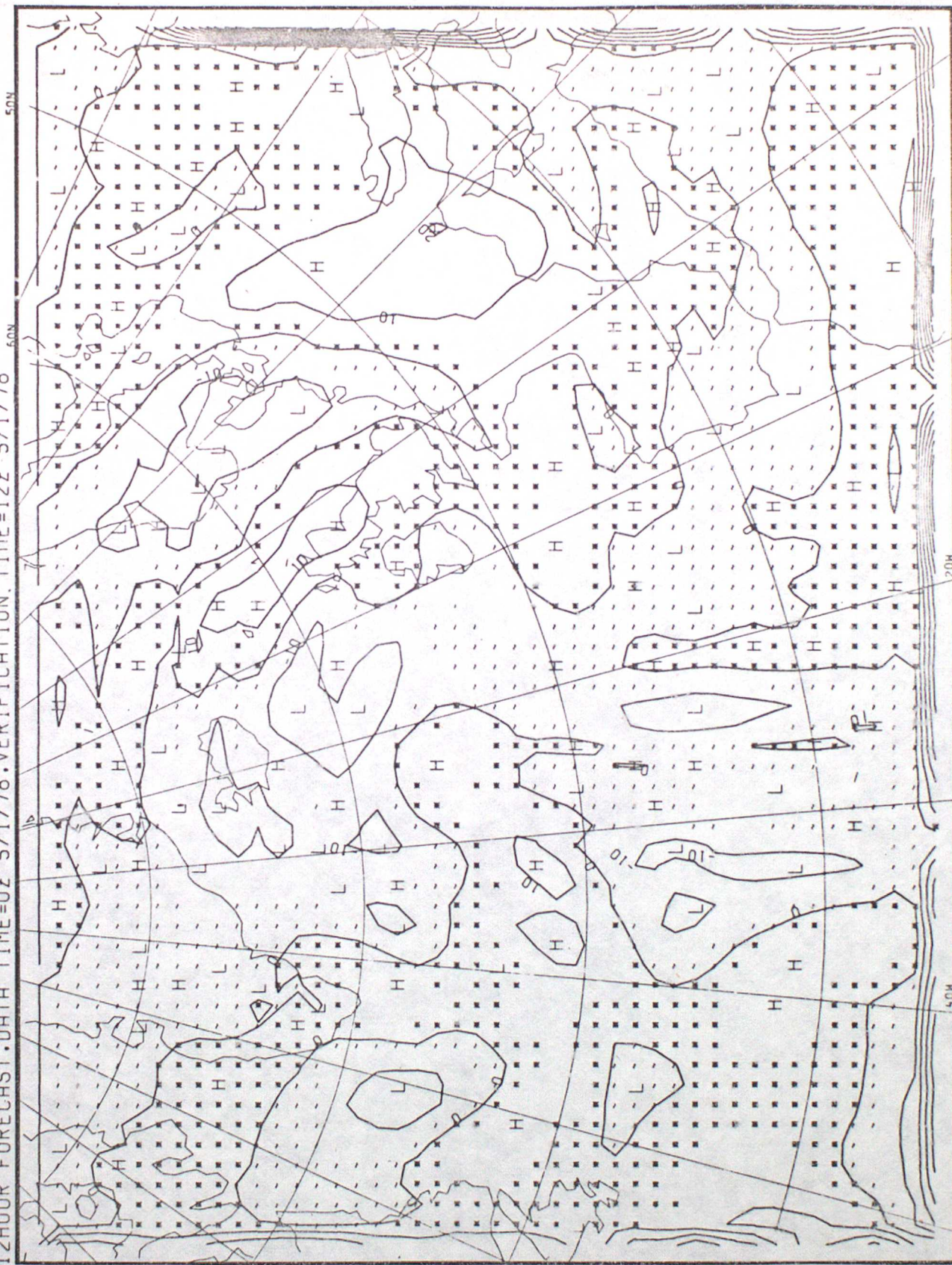


Figure 4a - the 550mb ω field before initialisation (dry forecast)

500MB VERT VEL. ISOPLETH INTERVAL=10 MB/HR

0000R FORECAST, DATA TIME=12Z 5/1/78, VERIFICATION TIME=12Z 5/1/78

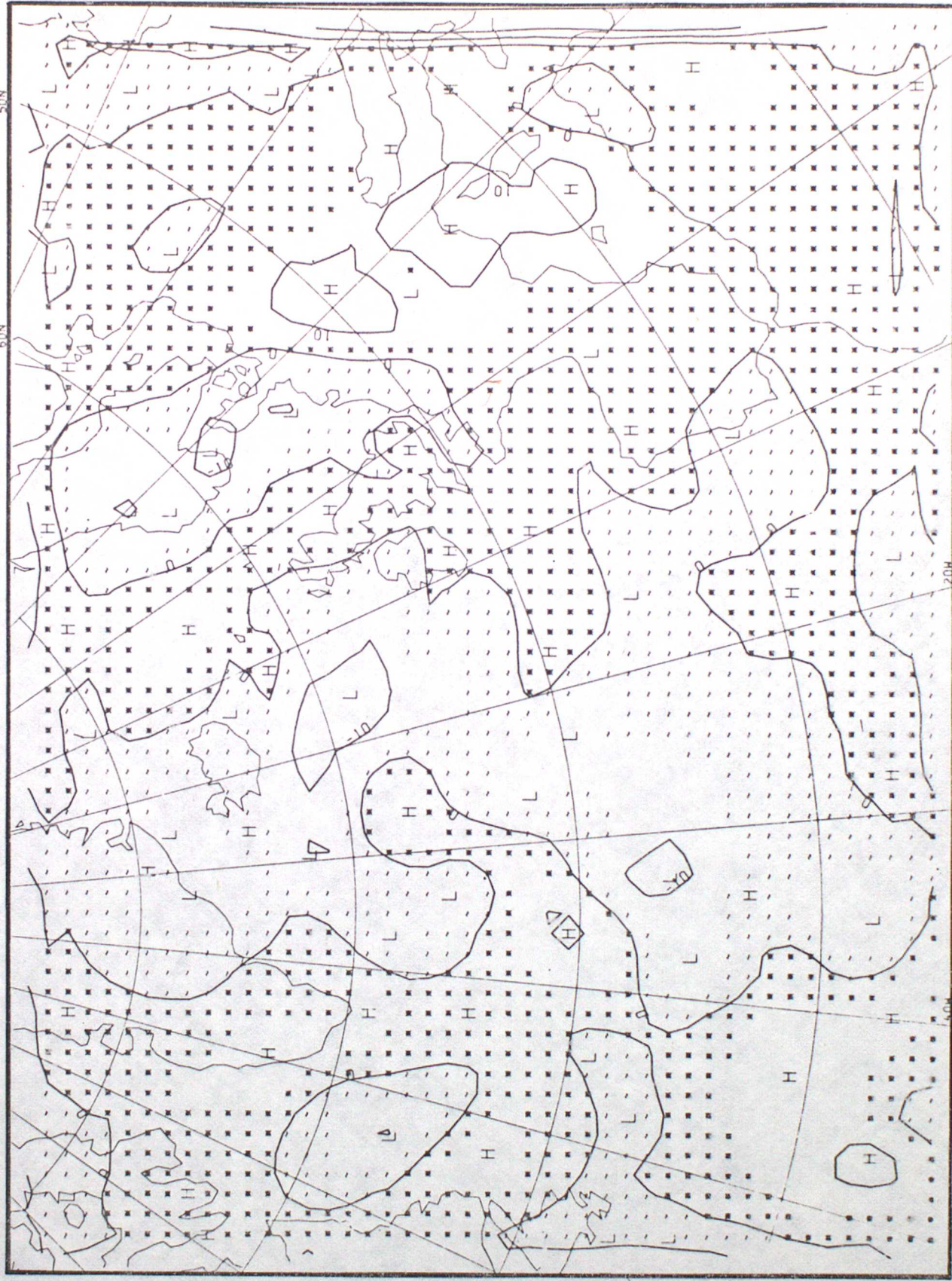


Figure 4b - the 550mb w field after initialisation (dry forecast)

HOURLY FORECAST DATA TIME=12Z 5/1/78. VERIFICATION TIME=12Z 5/1/78

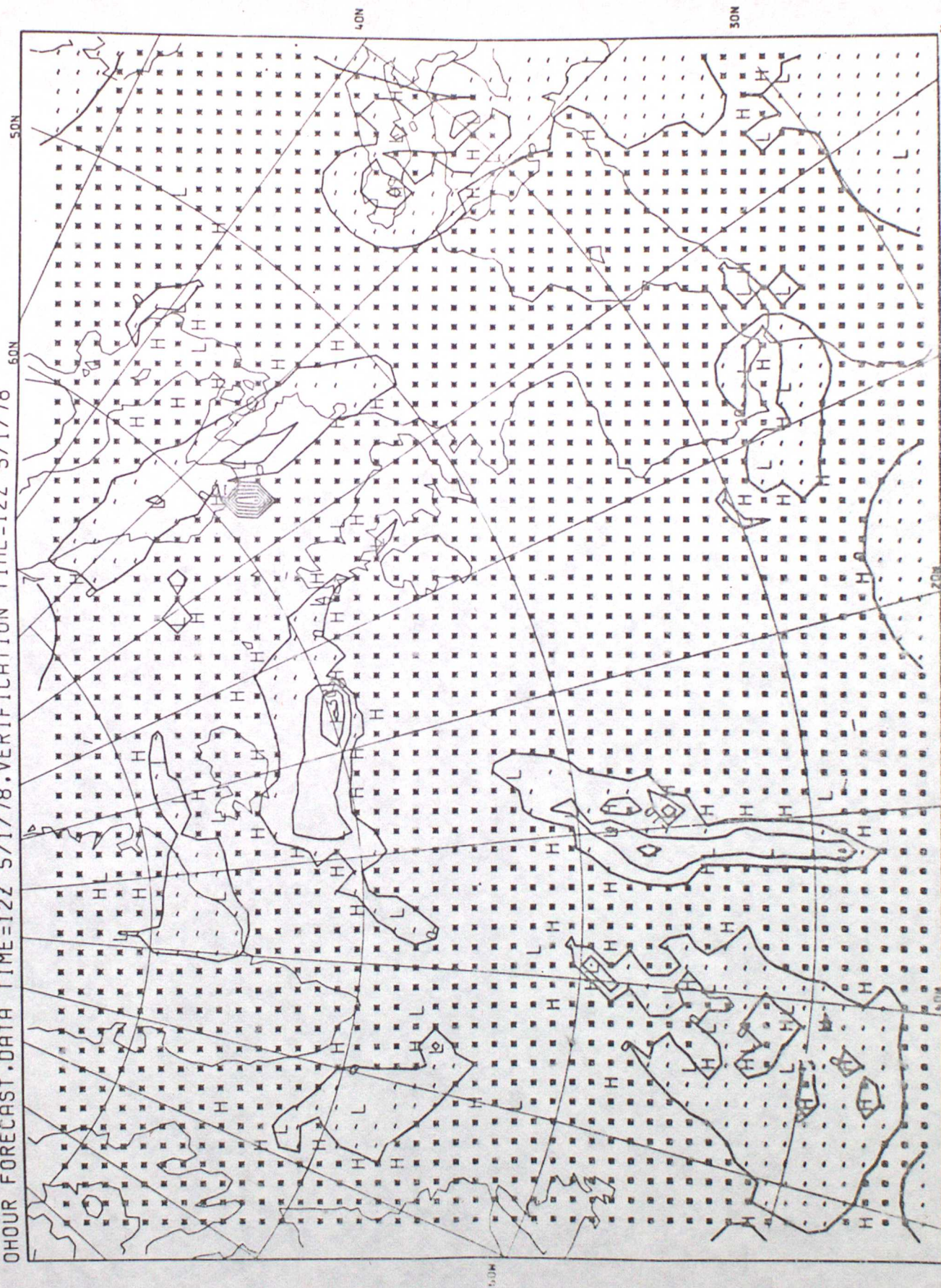


Figure 5a w_L - that part of the w field from the original 12 hr forecast that is related to the release of latent heat

ISOPLETH INTERVAL=10 MB/HR

12HOUR FORECAST. DATA TIME=0Z 5/1/78. VERIFICATION TIME=12Z 5/1/78

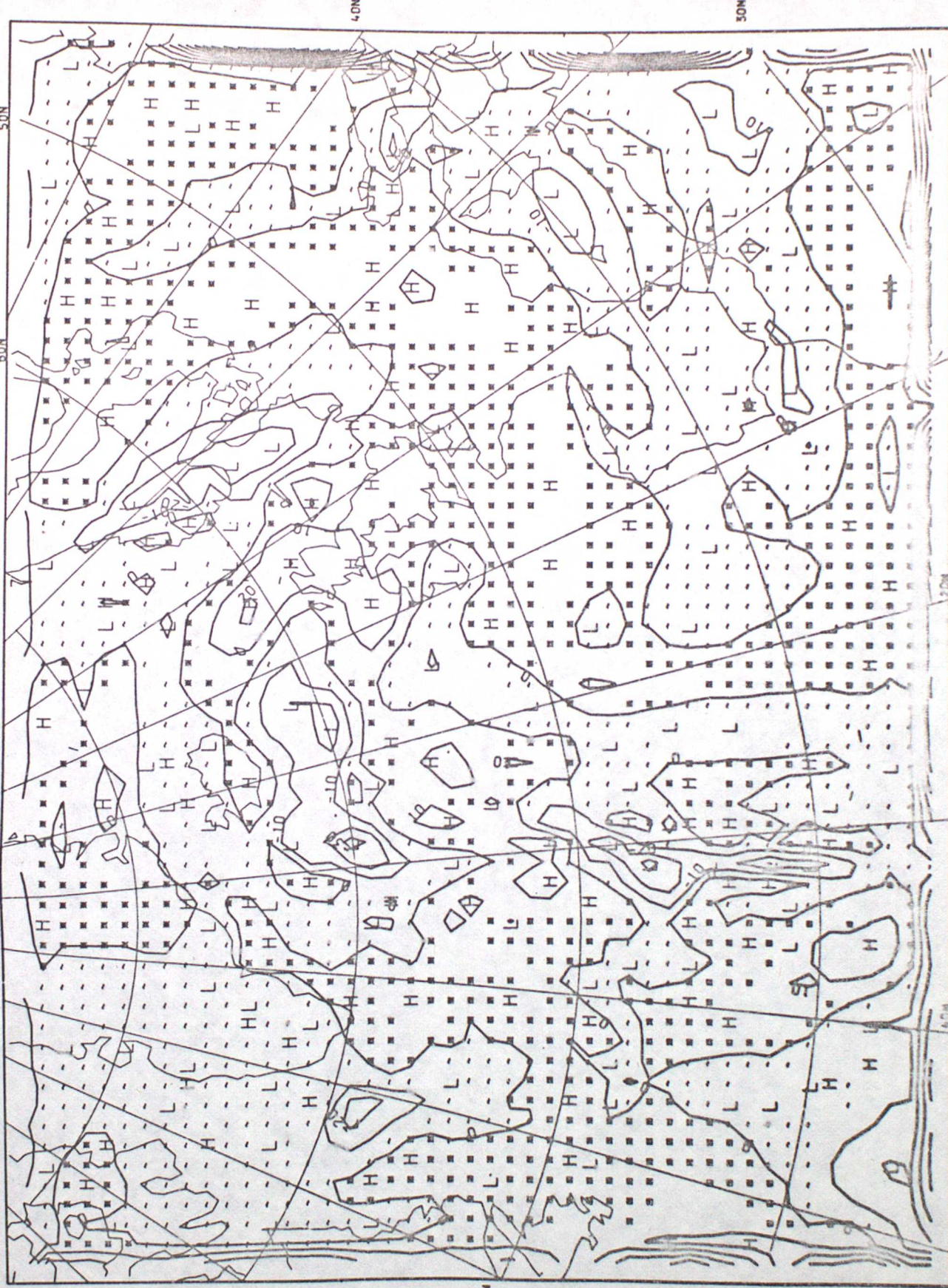


Figure 5b - the difference between the 550 mb w

FORECAST SURFACE PRESSURE AND PRECIPITATION

24 HOUR FORECAST, DATA TIME=0Z 5/1/78, VERIFICATION TIME=0Z 6/1/78

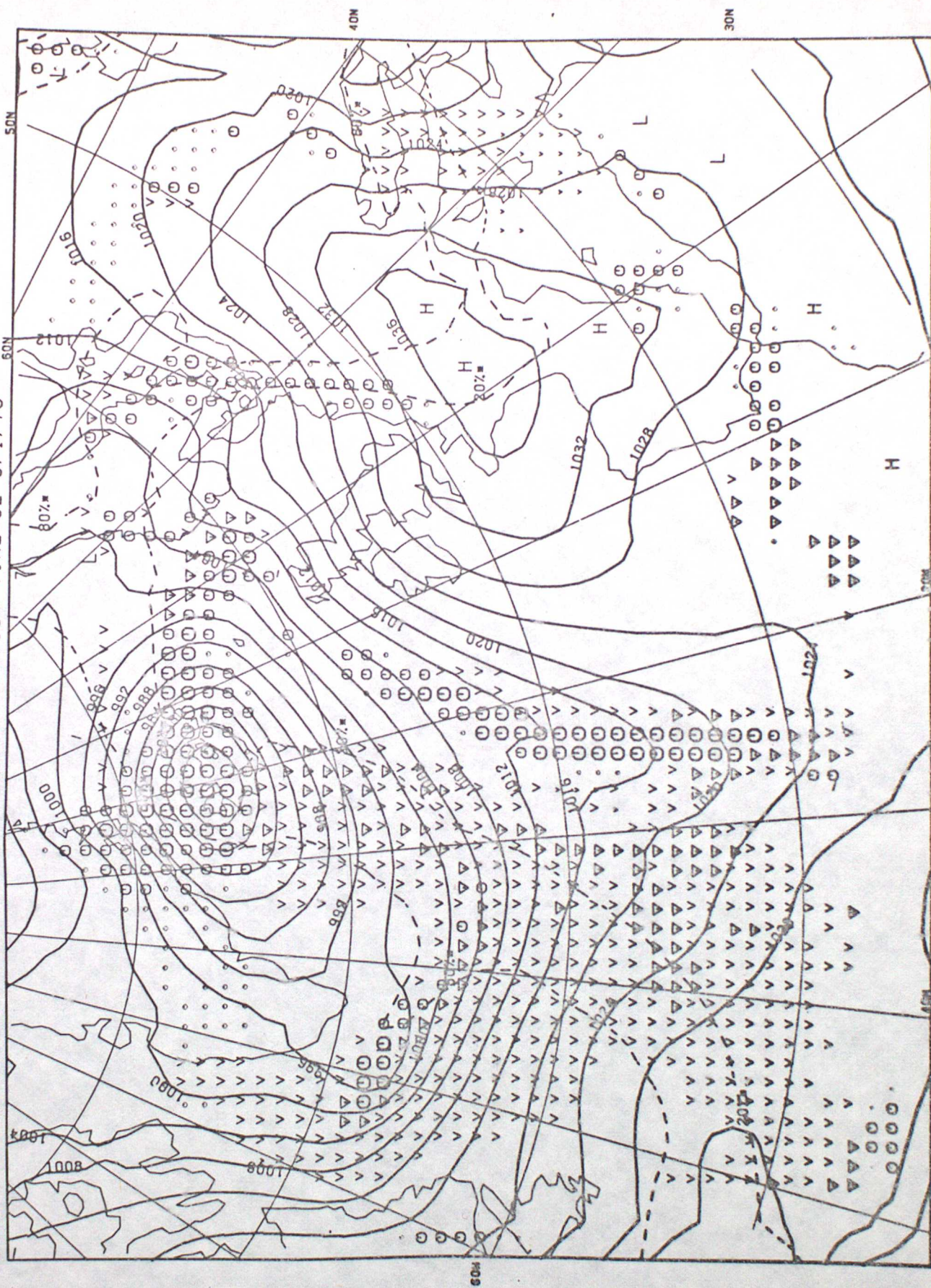


Figure 6a - a 12hr forecast from 12Z 5/1/78 using the original fields (i.e. a 12hr forecast from 00Z 5/1/78)

FORECAST SURFACE PRESSURE AND PRECIPITATION

12HOUR FORECAST .DATA TIME=12Z 5/1/78 .VERIFICATION TIME=0Z 6/1/78

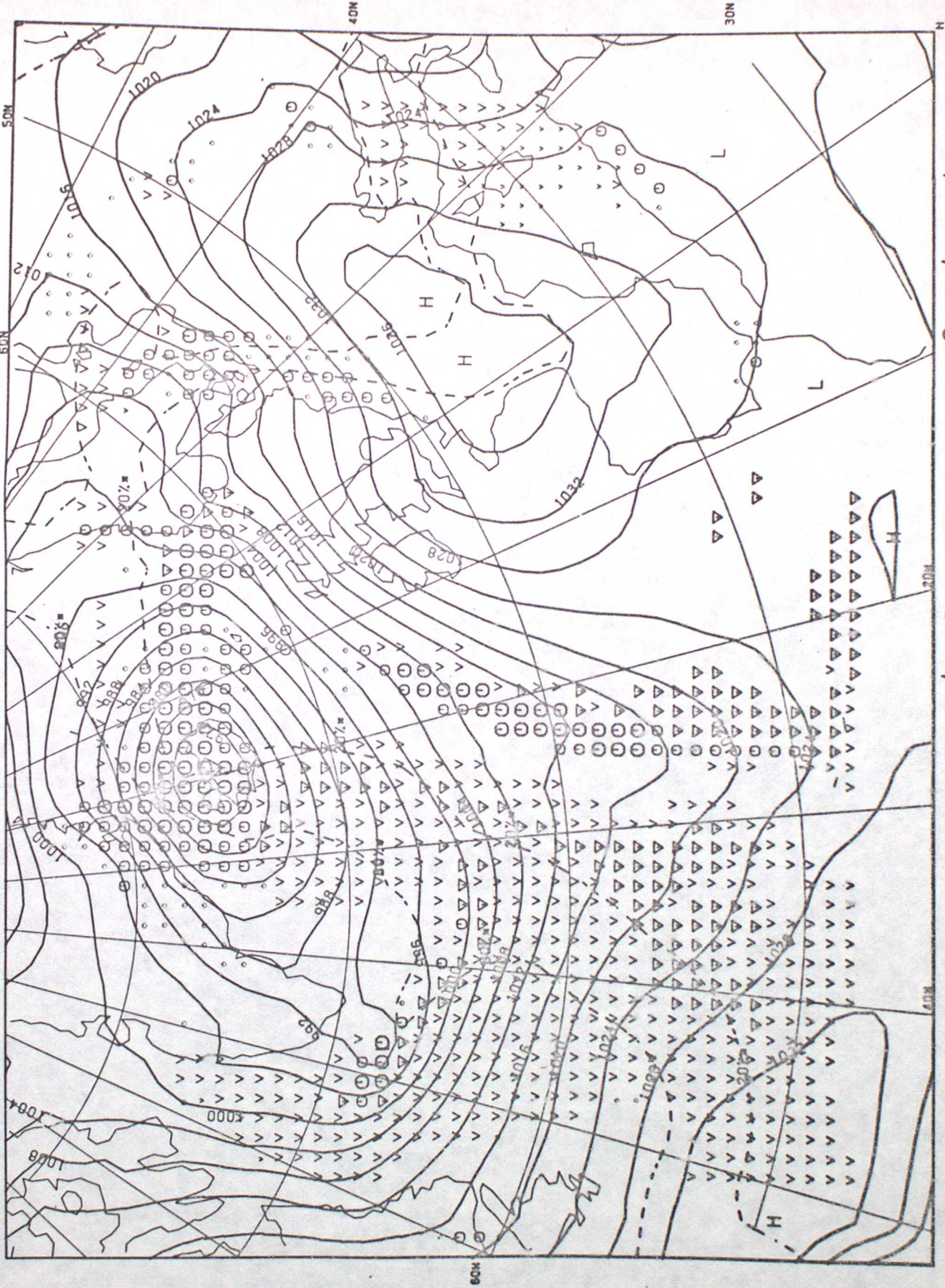


Figure 6b - a 12hr forecast from 12Z 5/1/78 using the newly initialised fields

RATE OF DYNAMIC RAIN

ISOPLETHS AT 0.5 MM/HR

24 HOUR FORECAST, DATA TIME=0Z 5/1/78, VERIFICATION TIME=0Z 6/1/78

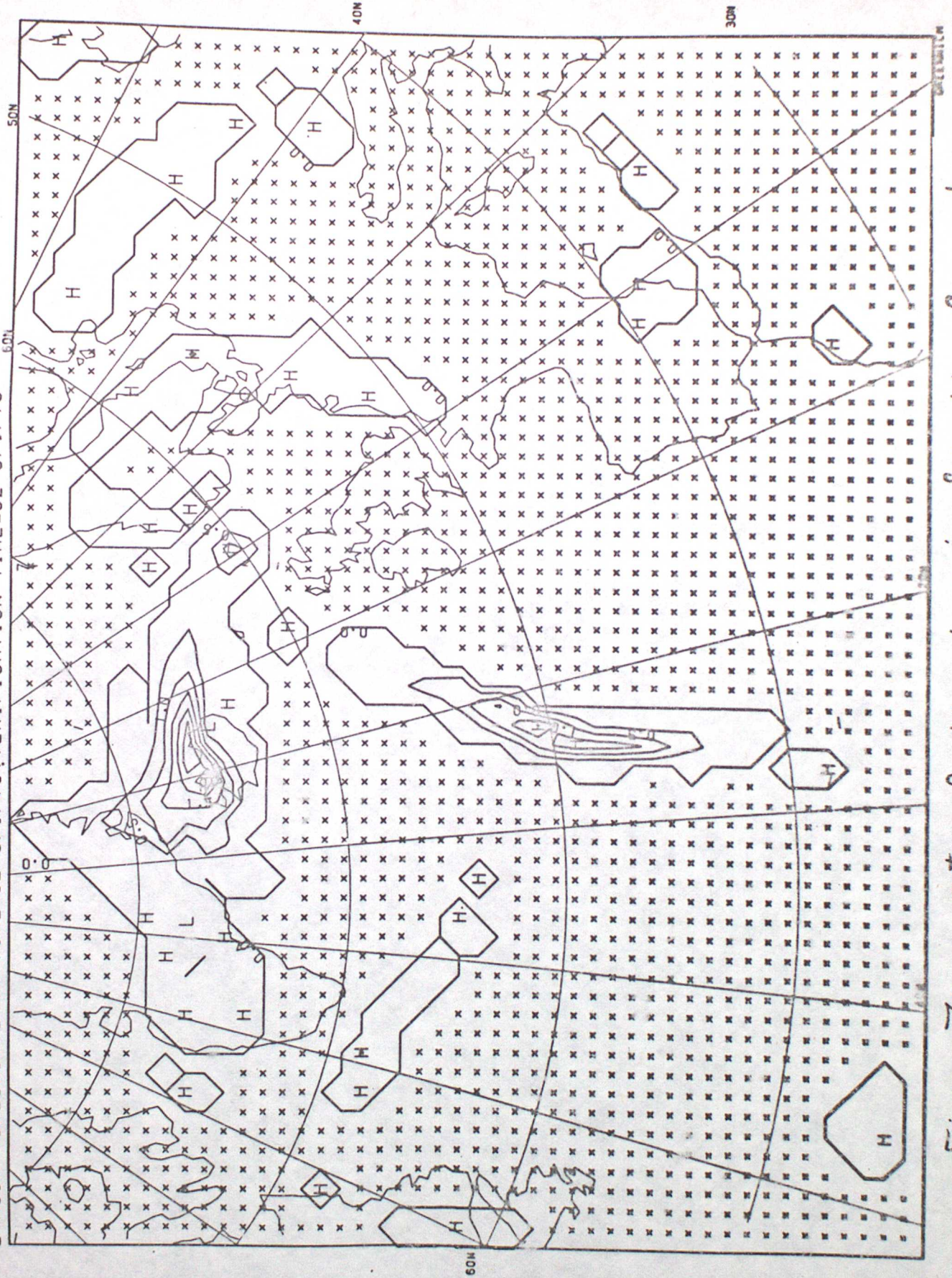


Figure 7a - rate of dynamic rain for the forecast shown in Figure 6a

RATE OF DYNAMIC RAIN

ISOPLETHS AT 0.5 MM/HR

12HOUR FORECAST, DATA TIME=12Z 5/1/78, VERIFICATION TIME=0Z 6/1/78

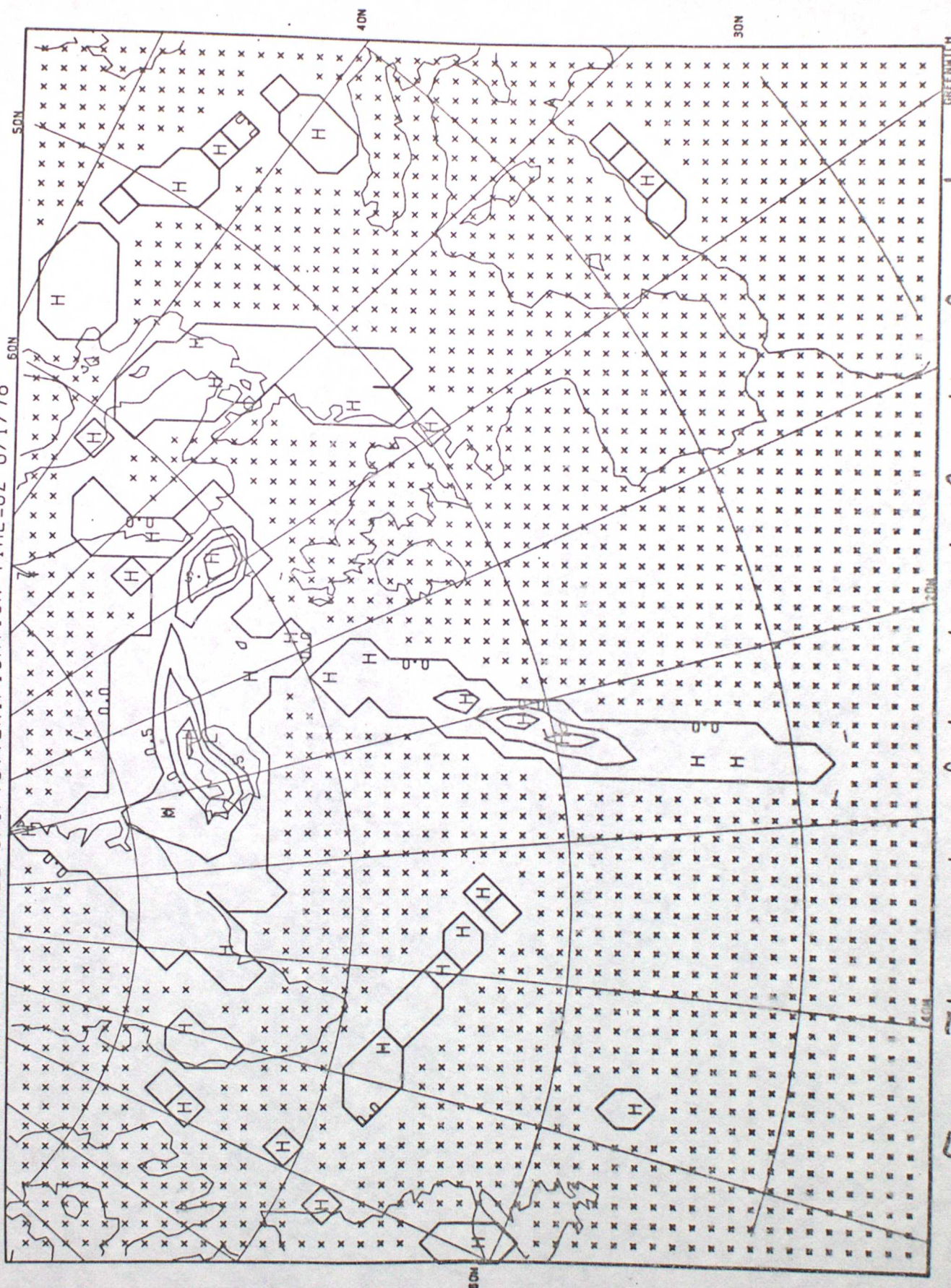


Figure 7b - rate of dynamic rain for the forecast shown in Figure 6b

500MB VERT VEL. ISOPLETH INTERVAL=10 MB/HR

24 HOUR FORECAST, DATA TIME=0Z 5/1/78, VERIFICATION TIME=0Z 6/1/78



Figure 8a - the 550mb w field corresponding to the forecast shown in Figure 6a.

500MB VERT VEL. ISOPLETH INTERVAL=10 MB/HR

12 HOUR FORECAST, DATA TIME=12Z 5/1/78, VERIFICATION TIME=0Z 6/1/78

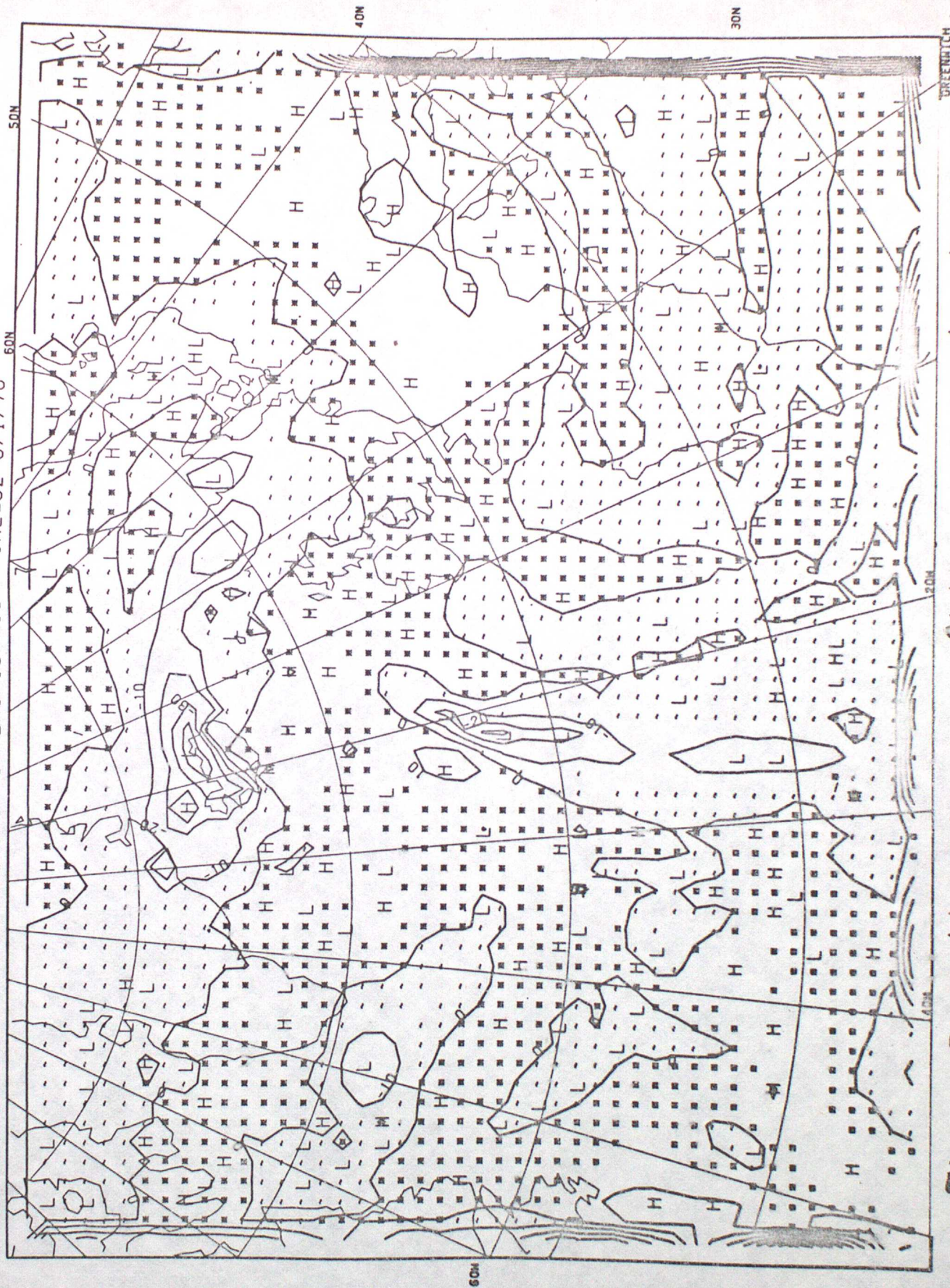


Figure 8b - the 550 mb w field corresponding to the forecast shown in Figure 6b

ACCUMULATED RAIN ISOHYETS AT 2 MM INTERVALS

VERIFICATION TIME=0Z 6/1/78

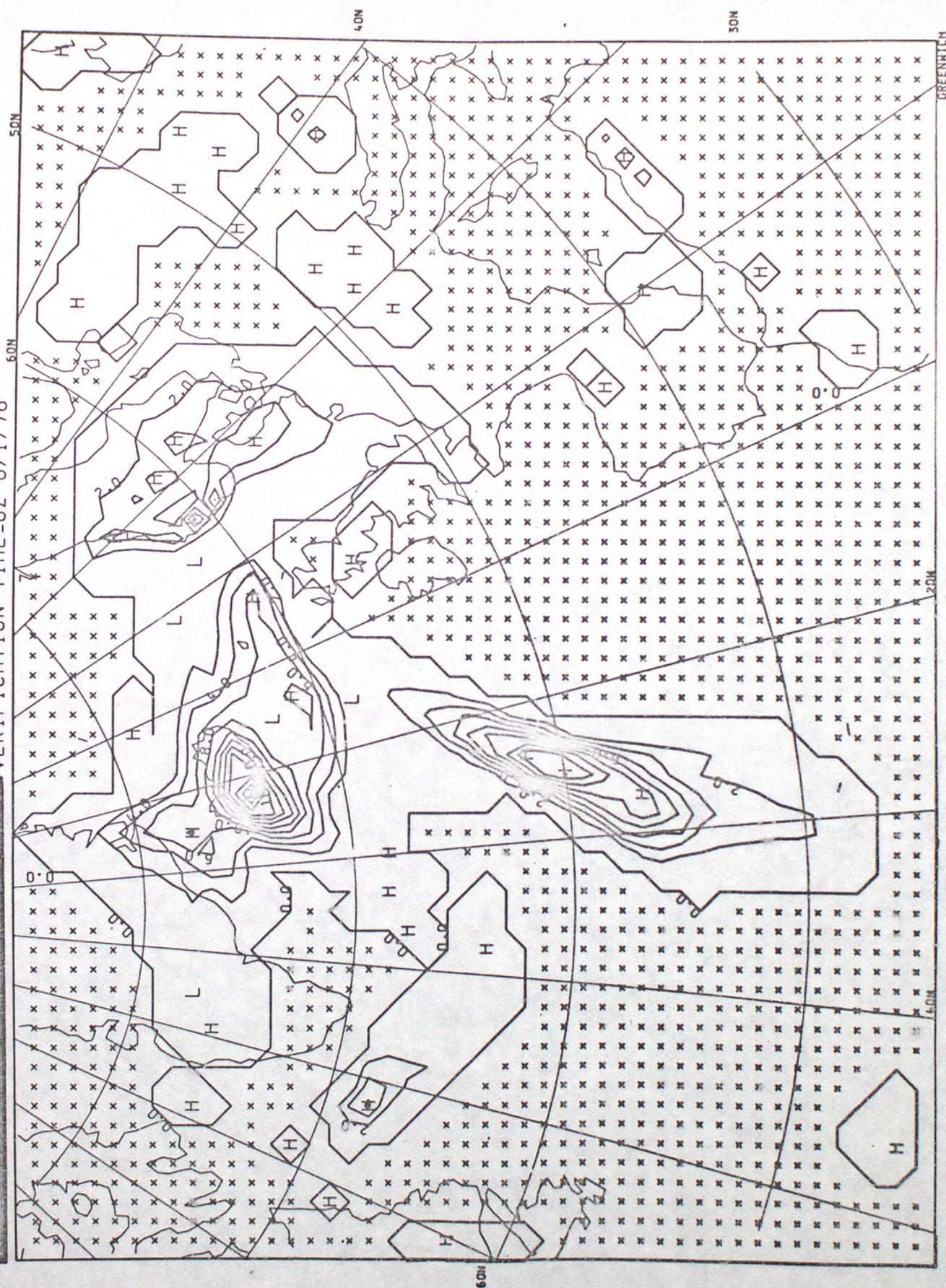


Figure 9a - accumulated dynamic rain between 12Z 5/1/78 and 00Z 6/1/78 for the original forecast

ACCUMULATED RAIN ISOHYETS AT 2 MM INTERVALS

VERIFICATION TIME=0Z 6/1/78

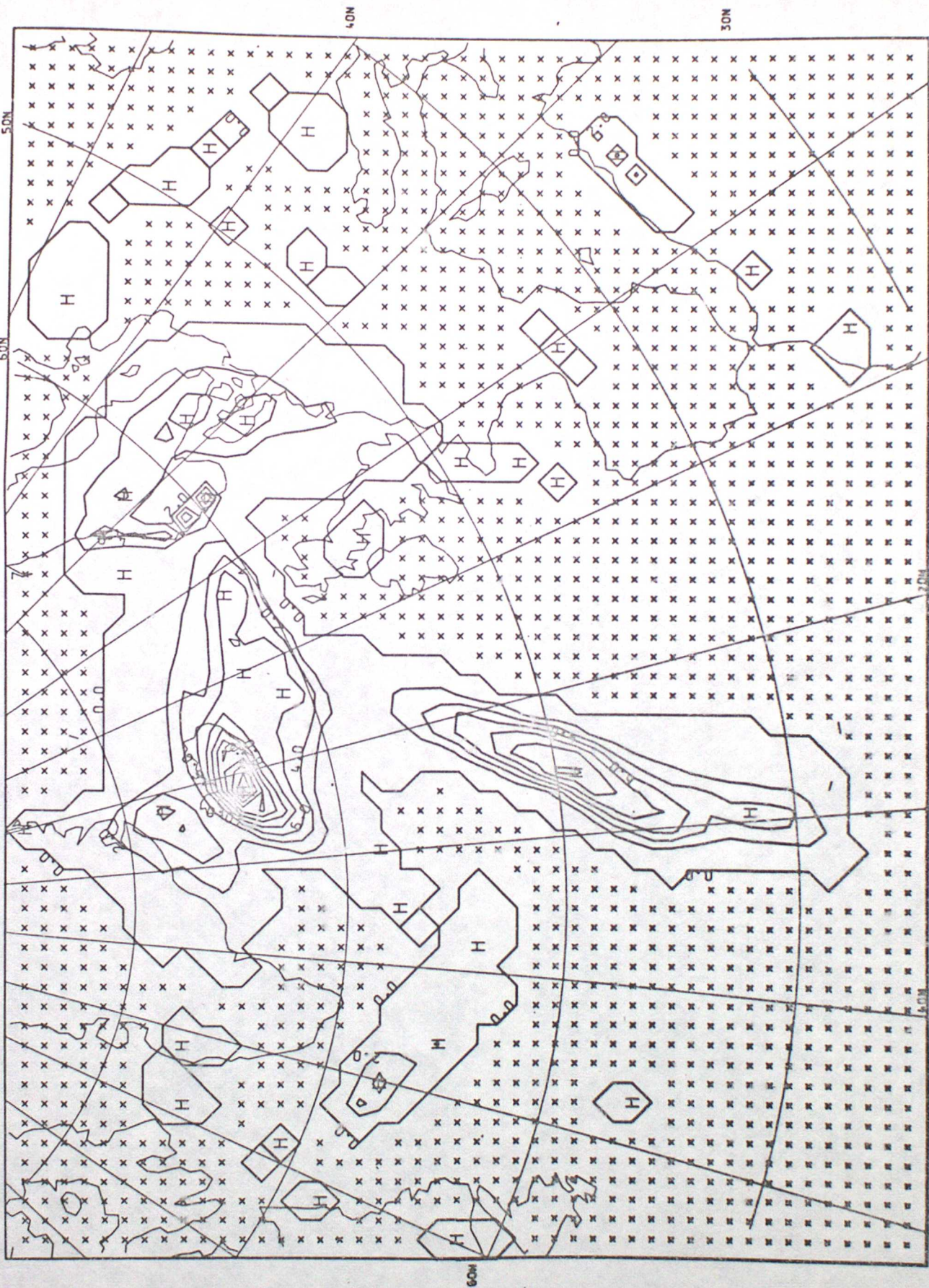


Figure 9b - accumulated dynamic rain between 12Z 5/1/78 and 00Z 6/1/78 for the forecast initialised at 12Z 5/1/78